Convective heat transport in stratified atmospheres at low and high Mach number

Evan H. Anders and Benjamin P. Brown
Department of Astrophysical & Planetary Sciences, University of Colorado – Boulder and Laboratory for Atmospheric and Space Physics, Boulder, CO

Here we study the effects of varying the strength of buoyant driving (the Rayleigh number, Ra) and the characteristic flow speed (the Mach number, Ma) on convective heat transport in stratified atmospheres. We utilize polytropic reference states to condition the Mach number and study the evolution of the non-dimensional Nusselt number (Nu) as Ra is increased in various Ma regimes.

INTRODUCTION

Convection is ubiquitous among natural systems such as stellar envelopes and planetary atmospheres. In these systems, compressibility and buoyancy couple to produce complex effects which are not seen in the widely-studied Rayleigh-Bénard convection. Early studies of stratified convection in two [1–4] and three [5–7] dimensions utilized polytropically stratified atmospheres, in which the equation of hydrostatic equilibrium is satisfied under the assumptions of constant gravitational acceleration, thermal diffusivity and a linear temperature profile. radiative transfer properties (cite some papers), the polytrope is a particularly useful reference state for stratified convection studies.

Aside from the physical size of the domain in which convection occurs, Rayleigh-Bénard convection has two main control parameters. These are the non-dimensional Rayleigh number (Ra, the ratio of buoyanty driving to diffusivity) and the Prandtl number (Pr, the ratio of viscous to thermal diffusivity). In stratified atmospheres, Ra and Pr combine with the degree of stratification of the atmosphere and the characteristic Mach number of motions in the convective flows. While there have been numerous studies of the effects of varying Ra, Pr, and atmospheric stratification (cite some), there are few studies of the effects of Mach number on the resulting heat transport properties of the resulting convection.

In this letter, we hold the Prandtl number and density stratification constant in polytropic atmospheres. We examine the effects of varying the Rayleigh number and characteristic superadiabaticity of the reference polytrope as a means of probing dynamics at low and high Mach number. We utilize the non-dimensional Nusselt number to study the heat transport characteristics at low and high Mach number.

MODEL & EQUATIONS

We study a fluid whose equation of state is that of an ideal gas, $P = R^*\rho T$ and whose initial stratification is polytropic. The primary assumptions utilized in constructing a polytropic atmosphere are that the gravitational acceleration and conductive heat flux are invariant throughout the depth of the atmosphere. In order to satisfy the latter assumption, the thermal conductivity, κ and temperature gradient ∇T_0 are often taken as constants, such that, $\boldsymbol{F}_{\rm cond} = -\kappa\nabla T_0 =$ constant. Under these assumptions, solving the equation of hydrostatic equilibrium produces an atmosphere defined by

$$\begin{aligned} \rho_0(z) &= \rho_{00}(z_0 - z)^m \\ T_0(z) &= T_{00}(z_0 - z) \end{aligned} \tag{1}$$

and z increases upwards within the bounds $z = \{0, L_z\}$. We specify the number of density scale heights the atmosphere spans, n_ρ to determine L_z. Throughout this study, we set $n_\rho = 3$ such that the density at the bottom of the atmosphere is larger than that at the top of the atmosphere by roughly a factor of 20. Thermodynamic variables are nondimensionalized at the top of the atmosphere as $P_0(L_z) = \rho_0(L_z) = T_0(L_z) = 1$, requiring $z_0 \equiv L_z + 1$ and $R^* = T_{00} = \rho_{00} = 1$. The polytropic index is set by the adiabatic index of a monatomic ideal gas, $\gamma = 5/3$ and the superadiabatic excess [1], ϵ, such that $m = (\gamma - 1)^{-1} - \epsilon = m_{ad} - \epsilon$ and the subsequent entropy gradient at the top of the atmosphere is $\nabla S(L_z) = -\epsilon$, the negative value of the superadiabatic excess.

Atmospheric diffusivities are set by the Rayleigh number and the Prandtl number. We define the non-dimensional Rayleigh number as

$$\mathrm{Ra} = \frac{gL_z^3(\Delta S_0/c_P)}{\nu\chi}, \tag{2}$$

where ΔS_0 is the entropy difference between the top and bottom of the atmosphere, ν is the kinematic viscosity (viscous diffusivity), and χ is the thermal difusivity. The relationship between the thermal and viscous diffusivities is set by the Prandtl number, Pr= ν/χ. We relate the dynamic viscosity, μ and the thermal conductivity, κ, to their corresponding diffusivities such that $\nu \equiv \mu/\rho$ and $\chi \equiv \mu rho$. As a result, Ra $\propto (\nu\chi)^{-1} \propto \rho^2$, such that for our atmospheres with $n_\rho = 3$, the Rayleigh number increases by a factor of approximately 400 from the top of the domain to the bottom of the domain. Such a formulation leaves Pr constant throughout the depth of the atmosphere, and in this paper we specifically study Pr = 1.

At the constant values of n_ρ and Pr used, the primary control parameters of convection are ϵ and Ra. We de-

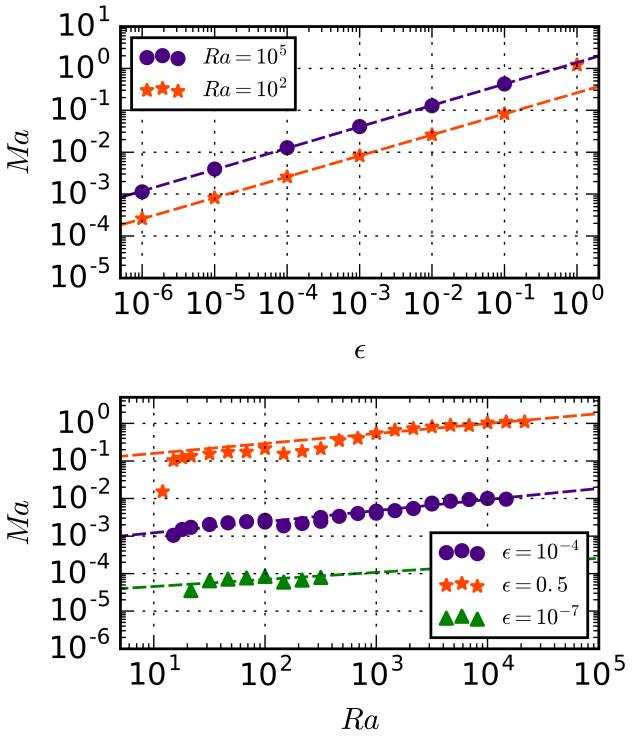

FIG. 1. Shown are characteristic mach numbers from IVPs spanning six decades of ϵ, from very low Mach number to near Mach one. A very strong Ma $\propto \epsilon^{1/2}$ relation is clear. (need to actually do linear regression)

compose our atmosphere into the background polytrope (ρ_0, T_0) and the fluctuations about that background $(\boldsymbol{u}, \rho_1, T_1)$. The scaling of the entropy gradient with ϵ is reflected in the evolved values of these fluctuations, which follow the scaling of $\mathrm{Ma}^{1/2} \propto T_1/T_0 \propto \rho_1/\rho_0 \propto \epsilon$, and which scale as roughly $Ra^{0.3}$, see Fig. 1.

We start with initial conditions of random small perturbations compared to ϵ in the temperature field. We evolve the Fully Compressible Navier-Stokes equations with an energy-conserving energy equation, which take the form:

$$\frac{D \ln \rho}{Dt} + \nabla \cdot (\boldsymbol{u}) = 0 \tag{3}$$

$$\rho \frac{D\boldsymbol{u}}{Dt} = -\nabla P + \rho \boldsymbol{g} - \nabla \cdot \bar{\bar{\boldsymbol{\Pi}}} \tag{4}$$

$$\rho c_V \left(\frac{DT}{Dt} + (\gamma - 1) T \nabla \cdot (\boldsymbol{u}) \right) + \nabla \cdot (-\kappa \nabla T) = - \left(\bar{\bar{\boldsymbol{\Pi}}} \cdot \nabla \right) \cdot \boldsymbol{u} \tag{5}$$

where $D/Dt \equiv \partial_t + \boldsymbol{u} \cdot \nabla$ and the viscous stress tensor is defined as

$$\Pi_{ij} \equiv -\mu \left(\frac{\partial u_i}{\partial x_j} + \frac{\partial u_j}{\partial x_i} - \frac{2}{3} \delta_{ij} \nabla \cdot (\boldsymbol{u}) \right). \tag{6}$$

In such stratified systems, the total convective flux can be defined as

$$\boldsymbol{F}_{\mathrm{conv}} = \boldsymbol{F}_{\mathrm{enth}} + \boldsymbol{F}_{\mathrm{KE}} + \boldsymbol{F}_{\mathrm{PE}} + \boldsymbol{F}_{\mathrm{visc}}, \tag{7}$$

where $\boldsymbol{F}_{\mathrm{enth}} \equiv \rho \boldsymbol{u}(c_V T + P/\rho)$ is the enthalpy flux, $\boldsymbol{F}_{\mathrm{KE}} \equiv \rho |\boldsymbol{u}|^2 \boldsymbol{u}$ is the kinetic energy flux, $\boldsymbol{F}_{\mathrm{PE}} \equiv \rho \boldsymbol{u} \phi$ is the potential energy flux (with $\phi \equiv -gz$), and $\boldsymbol{F}_{\mathrm{visc}} \equiv \boldsymbol{u} \cdot \bar{\bar{\boldsymbol{\Pi}}}$ is the viscous flux. Dotting Eq. 4 with $\boldsymbol{u}$ and adding it to Eq. 5, we retrieve the full energy equation in conservation form,

$$\frac{\partial}{\partial t} \left(\rho \left[\frac{|\boldsymbol{u}|^2}{2} + c_V T + \phi \right] \right) + \nabla \cdot (\boldsymbol{F}_{\mathrm{conv}} + \boldsymbol{F}_{\mathrm{rad}}) = 0 \tag{8}$$

where $\boldsymbol{F}_{\mathrm{rad}} = -\kappa \nabla T$.

The efficiency of convection is defined by the Nusselt number. While the Nusselt number is well-defined in Rayleigh-Bénard convection as the amount of total flux divided by the steady-state background conductive flux [9, 10], a well-defined Nusselt number is more elusive in stratified convection. A traditional definition of the Nusselt number in stratified convection is [1**?**]

$$N \equiv \frac{F_{\mathrm{conv,\,z}} + F_{\mathrm{rad,\,z}} - F_A}{F_{\mathrm{ref}} - F_A}, \tag{9}$$

where $F_{\mathrm{conv,\,z}}$ and $F_{\mathrm{rad,\,z}}$ are the z-components of $\boldsymbol{F}_{\mathrm{conv}}$ and $\boldsymbol{F}_{\mathrm{rad}}$, respectively. F_A is the adiabatic conductive flux, defined as $F_A = -\kappa \nabla T_{\mathrm{ad}}$. For an atmosphere in hydrostatic equilibrium, such as a polytrope, $\nabla T_{\mathrm{ad}} \equiv -g/c_P$, and thus $F_A = \kappa g / c_P$. $F_{\mathrm{ref}} = \Delta T / L_z$ is the conductive flux of a linear profile connecting the upper and lower plates, where $\Delta T = T_u - T_\ell$.

Such a definition of the Nusselt number is general to both stratified and Rayleigh-Bénard convection. Convection works to suppress entropy stratification and create isentropic atmospheres. Under the Boussinesq approximation where density variations are ignored, entropy stratification is directly proportional to temperature stratification, such that $\nabla S \to 0$ only when $\nabla T \to 0$. Thus, for Rayleigh-Bénard convection, $\nabla T_{\mathrm{ad}} \equiv 0$ and the familiar form of N is retrieved. In the case of stratified convection, as $\epsilon \to m_{ad} + 1$, as in [**?**], $\nabla P \propto g \to 0$ and the resulting $\nabla T_{\mathrm{ad}} \to 0$. In such a case, $F_A \to 0$ and the familiar definition of the Rayleigh-Bénard nusselt number is appropriate to use. However, for any given values of ϵ, including the very small values used in this work, Eq. 9 is the proper non-dimensional definition of the Nusselt number.

WE USE DEDALUS, EXPLAIN WHAT IT ARE

EXPLAIN BOUNDARY CONDITIONS

EXPLAIN WHAT THE CHARACTERISTIC TIME SCALE, THE BUOYANCY TIME, IS

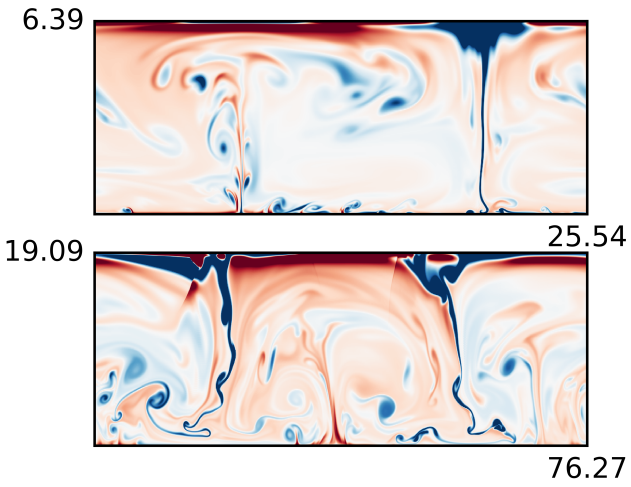

FIG. 2. Two characteristic snapshots after about 200 buoyancy times are shown at $\epsilon = 10^{-4}$ (top) and $\epsilon = 0.5$ (bottom) at Ra $= 10^6$.

RESULTS

We ran initial value problems for a few hundreds of buoyancy times past the convective transients from Rayleigh numbers around R_{crit} up to Rayleigh numbers of $\approx 10^7 R_{crit}$. While bulk thermodynamic structures are similar between low and high ϵ, high ϵ runs start to exhibit shock fronts propagating away from downflow channels, such as those in Fig. 2, as reported in [4].

Despite diferent thermodynamic structures, the fluxes look fairly similar at low and high mach number (sort of? I don't think the ones I have are averaged over enough time, especially the eps=0.5 one, but I Pleiades is a bit slammed right now). See Fig 3

At low Rayleigh number, diffusivities are high and the flows are very laminar. Such flows often achieve a steady state and have a well-defined Nusselt number which is independent of time. However, as the Rayleigh number increases, the flows become increasingly time-dependent. Even steady structures such as solid "rolls" like those pictured in Fig. 2 have highly time-dependent Nusselt numbers. This is, in part, due to the fact that cold downdrafts floating to the bottom of the domain can be entrained by upflows, or warm risen parcels can be entrainedi n the intense cold downdrafts. Such events reverse the preferred direction of flux in the system, and even let the Nusselt number become negative for short periods of time. See Fig. 4. As a result, it is necessary to take a long time average of the fluxes before calculating the Nusselt number at higher Rayleigh number.

The evolution of the Nusselt number as the Rayleigh number is increased is shown for both high and low ϵ in Fig. 5. Below convective onset, the Nusselt number is perfectly one. Just above onset, there is a brief range of highly inflated scaling between N and Ra. From about $10R_{crit}$ to roughly $10^{4-5}R_{crit}$, Ra and N follow the relationship: (put a power law here) Above about $10^5 R_{crit}$, the Nusselt number flattens out as Ra is increased – perhaps this is some Featherstone 2016 shennanigans.

This work was supported by the CU/NSO Hale Graduate Fellowship and Juri's allocation and Ben's allocation.

[1] E. Graham, Journal of Fluid Mechanics **70**, 689 (1975).
[2] K. L. Chan, S. Sofia, and C. L. Wolff, Astrophys. J. **263**, 935 (1982).
[3] N. E. Hurlburt, J. Toomre, and J. M. Massaguer, Astrophys. J. **282**, 557 (1984).
[4] F. Cattaneo, N. E. Hurlburt, and J. Toomre, ApJL **349**, L63 (1990).
[5] A. Malagoli, F. Cattaneo, and N. H. Brummell, ApJL **361**, L33 (1990).
[6] F. Cattaneo, N. H. Brummell, J. Toomre, A. Malagoli, and N. E. Hurlburt, Astrophys. J. **370**, 282 (1991).
[7] N. H. Brummell, N. E. Hurlburt, and J. Toomre, Astrophys. J. **473**, 494 (1996).
[8] A. Brandenburg, K. L. Chan, Å. Nordlund, and R. F. Stein, Astronomische Nachrichten **326**, 681 (2005), astro-ph/0508404.
[9] H. Johnston and C. R. Doering, Physical Review Letters **102**, 064501 (2009), 0811.0401.
[10] J. Otero, R. W. Wittenberg, R. A. Worthing, and C. R. Doering, Journal of Fluid Mechanics **473**, 191 (2002).

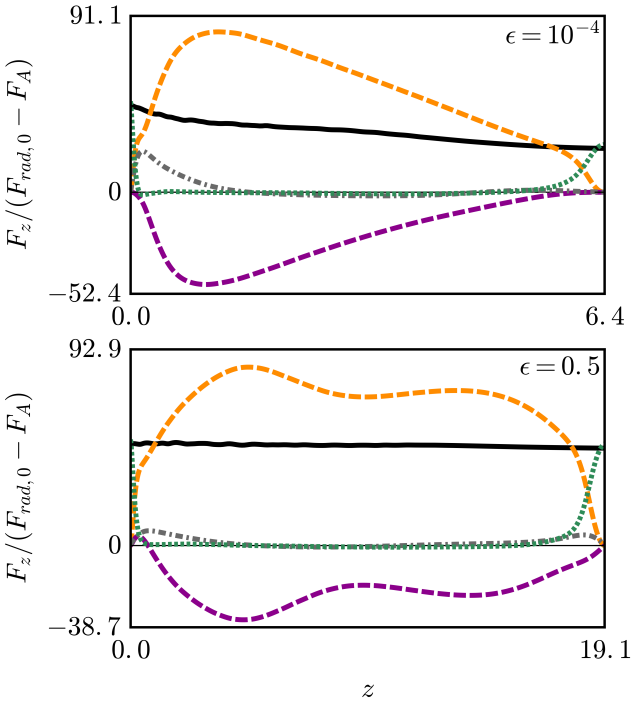

FIG. 3. Flux profiles for low (top) and high (bottom) Mach number flows.

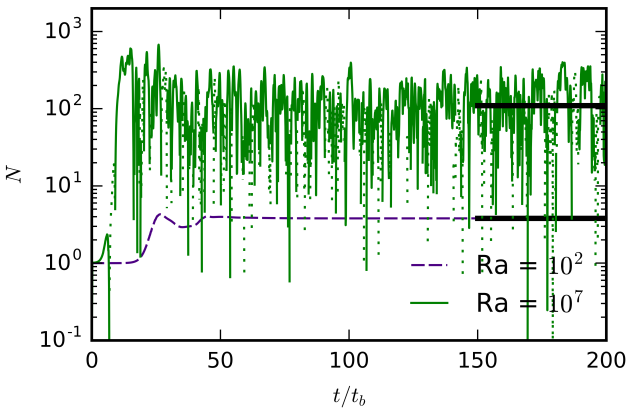

FIG. 4. The evolution of the Nusselt number is shown at low (10^2) and high (10^7) Rayleigh number and at $\epsilon = 10^{-4}$. At low Rayleigh number, the system is able to settle into a time invariant solution. As the Rayleigh number is raised, the thermodynamic structure become increasingly complex and time variant, and a time-average of the Nusselt number is required to obtain a sensible mean.

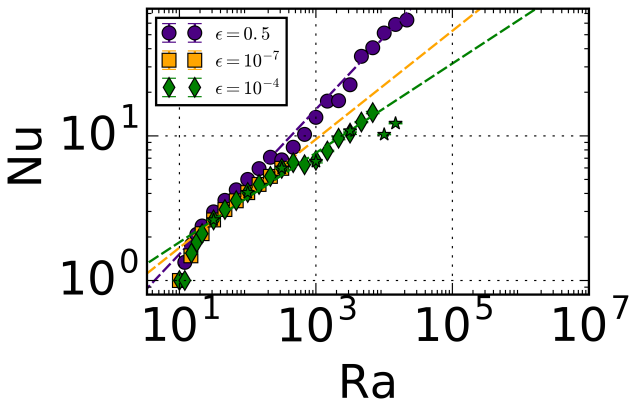

FIG. 5. Variation of the Nusselt number as a function of the Rayleigh number is shown.